Egyptian Journal of Archaeological and Restoration Studies (*EJARS*)
An international peer-reviewed journal published bi-annually
www.ejars.sohag-univ.edu.eg

*Original article*

# ANALYTICAL AND CONSERVATION TECHNIQUES OF A GRECO ROMAN *BOS TAURUS* CRANIUM

Abdel-Maksoud, G.[1(*)], Wahid, E.[2], Abdel-Aziz, M.[3], Elserogy, A.[4] & Abdel Wahab, T.[5]

[1]*Organic Materials Conservation dept., Faculty of Archaeology, Cairo Univ., Giza, Egypt.*
[2]*Conservator, graduated from Conservation dept., Faculty of Archaeology, Cairo Univ., Giza, Egypt.*
[3]*Microbial Chemistry dept., Biotechnology Research Institute, National Research Centre, Dokki, Giza, Egypt.*
[4]*Conservation dept., Faculty of Archaeology, Fayoum Univ., Fayoum, Egypt.*
[5]*Anthropology dept., Faculty of African Postgraduate Studies, Cairo Univ., Giza, Egypt.*
**E-mail address: gomaa2014@cu.edu.eg*

**Article info.**
**Article history:**
Received: 16-3-2023
Accepted: 13-8-2023
Doi: 10.21608/ejars.2024.361163

**Keywords:**
*Greco-Roman period*
*Bos taurus*
*Cranium*
*Deterioration*
*Analytical techniques*
*Conservation methods*

EJARS – Vol. 14 (1) – June. 2024: 1-10

**Abstract:**
*The Agricultural Museum is considered one of the most important museums in Egypt. It contains many different archaeological materials, especially osteological remains. The studied cranium dates back to the Greco-Roman period and suffers from deterioration. The aim of the study was to utilize different analytical techniques in evaluating the state of preservation of the sample and applying required conse-rvation methods. The analytical techniques used were photographic documentation, digital microscope, scanning electron microscope (SEM), polarized light microscope, attenuated total reflectance/Fourier Transform Infrared (ATR/FTIR), color change using spectrophotometer, contact angle, and isolation and identification of fungi. The results of the analytical techniques revealed that the cranium was suffering from adverse deterioration (such as a change in the chemical composition, change of color, deterio-ration of surface morphology, low contact angle and the most occurrence fungi were Penicillium chrysogenum, Aspergillus niger, Aspergillus terreus, and Cladosporium cladosporioides. The conservation methods applied were mechanical and chemical cleaning, consolidation, disi-nfection, and display of the cranium on new Plexiglas support. The conservation methods revealed the aesthetic value of the cranium.*

## 1. Introduction

Bone contains both organic and inorganic phases with a complex, yet well-known hierarchical structure. It consists of approximately 30% organic material, mainly type I collagen, 60% inorganic non-stoichiometric hydroxyapatite (bioapatite), and 10% water. Non-stoichiometry of bioapatite originates from the replacement of calcium or phosphate ions and hydroxyl groups by carbonates, which represent 3-5% of the weight of bioapatite [1-5]. The degradation of one of the bone components influences the degradation pathway of the other components by enhancing the access to solvents, oxygen, and microbes. The collagen is mainly degraded by microorganisms even if chemical hydrolysis may occur, and hydroxyapatite is mainly degraded or recrystallized through chemical dissolution [6]. Deterioration, both microbiological and biochemical (autolysis) of tissue begins immediately after death, with the soft tissues usually showing the effects first [7]. Once the bones enter the burial environment after death, they go through several processes that can lead to their deterioration. These processes are chemical, physical, and biological. They can be obtained from intrinsic and extrinsic factors [8,9]. Intrinsic factors include human or animal age, as small-age bones decompose faster than large-age bones in the same environment [10,11]. Bone type and size play a significant role in the process of damage, as cancellous bones are faster to decompose than compact bones [12]. Also, pathological conditions and injuries are known to speed up the decomposition of buried bone [13]. Porosity and bone density are considered one of the most important intrinsic factors, as more porous tissues decay more rapidly than less porous tissue [14,15]. Extrinsic factors include groundwater, which plays an important role in the deterio-ration of archaeological bone. The presence of water in the burial environment will lead to increased solubility and bone loss. Groundwater is also the medium for many other pro-

cesses such as ion exchange, recrystallization, ion exchange, and biological attack [16-18]. Increasing or decreasing temperature is an important factor in the deterioration of archaeological bones. High temperature increases chemical reactions, and microorganism and insect activity. Low temperature leads to the formation of ice crystals and the destruction of cell structure [19,20]. The pH value and soil type detect the preservation or deterioration of archaeological bones. The acidic pH value leads to the solubility of the inorganic part in the bones. The bone is preserved in soil with a neutral or slightly alkaline pH value [21]. Flora and fauna, plant roots, human impact, and grave depth can play an important role in the deterioration of archaeological bone in the burial environment [9]. It can also be stated that inappropriate museum and storage environments (exposure to light, fluctuation between relative humidity and temperature, pollution, etc.) can also lead to the deterioration of archaeological bones. The analysis and investigation of archaeological bones extracted from excavations or found in museums are among the important steps in long-term conservation. Effective analysis determines the degree of sample deterioration, as well as the materials and methods that can be utilized in the conservation processes [22-24]. Conservation treatment becomes necessary and vital to reduce or stop the deterioration of the archaeological material and to improve or increase its chemical stability. The conservator should consider that the best treatment is the least treatment. Accordingly, the conservator should carry out the required conservation process only. This process should be based on the results of analyses and investigations so that the required treatment methods and appropriate materials can be selected and applied with them so that the originality of the treated material is preserved [25]. The current study aims to assess the condition of the studied cranium, using some types of advanced analytical techniques. The study also aims to apply some materials and methods of conservation treatment on the cranium to be an example that can be applied to the rest of the crania that date back to the same era as the studied cranium showing similar aspects of deterioration.

## 2. Materials and Methods

### 2.1. *Materials*

#### 2.1.1. Preparation of the new sample

A modern *Bos taurus* cranium was used as a reference sample. It was prepared after some references [26,27]. A cow cranium was brought from the butcher. The remains of fats, meat, and other impurities were cleaned using scalpels without any effects on the surface. Bone samples were left to dry naturally at room temperature (22 ºC±2 ºC) for one week.

#### 2.1.2. Archaeological sample

The studied cow's cranium was dated back to the Greco-Roman period. It is deposited in the Agriculture Museum in Giza, Egypt. Animals in ancient Egypt were recognized as tribal gods and were important in the performance of religion during the Egyptian kingdoms in particular in the late and subsequent ages. Perhaps one of the distinctive characteristics of Egyptian gods was the heads of birds and animals. The cow is associated with the goddess Hathor, a goddess with the body of a woman and the head of a cow and is considered a symbol of beauty, love, and happiness.

### 2.2. *Methods*

#### 2.2.1. Photographic documentation (morphometric assessment)

Aspects of deterioration detected on the surface of the studied cranium were visually assessed and then photographed using a digital camera (Samsung camera 38MP, f/2.2 lens slot) [28].

#### 2.2.2. Digital light microscope

The portable USB digital microscope (model PZ01-Shenzhen Super Eyes Co. Ltd., China) was used to examine the surface of the new and archaeological bone samples [29].

#### 2.2.3. Scanning electron microscope

The investigation of the surface morphology of **new** and archaeological bones was performed using SEM (Quanta 3D 200i made by FEI, accelerated voltage of 20.00 kV, and a magnification range of 250 to 2000X. The SEM investigation was done in the Grand Egyptian Museum - Conservation Center (GEM.CC), Cairo, Egypt.

#### 2.2.4. Polarized light microscope

Thin sections of new and archaeological samples were prepared according to Abdel-Maksoud [26]. Transverse sections were cut using a diamond-tipped saw, then ground by hand to a thickness of approximately 50 mm and polished. All thin sections were examined and studied using transmitted and polarizing light microscopy. Each section was viewed at several Magnifications and digitally photographed. The ZEISS Imager.A1m (Polarized Light Microscope: Axio vision 4.7 software; Camera Axiocam MRc5.).

#### 2.2.5. Attenuated total reflectance/fourier transform IR

The molecular structure of the studied samples was elucidated in the range 4000 to 400 $cm^{-1}$ by attenuated total reflection-Fourier transform infrared spectroscopy (ATR-FTIR), Bruker Vertex 70 FTIR spectrometer at the Molecular Modelling and Spectroscopy Unit, National Research Centre, Egypt. The calculation of carbonate content of new and archaeological bone was monitored through the $CO_3/PO_4$ parameter, calculated by dividing the intensity of the band at 1415 $cm^{-1}$ ($\nu3(CO_3)$ vibrational mode) by the intensity of the phosphate peak at 604 $cm^{-1}$ [30]. The crystallinity index of new and archaeological samples was calculated according to some references [31-33] as follows: Crystallinity index = (a+b)/c, Where:

**a**= height of the absorption peaks at 603 $cm^{-1}$.

**b=** height of the absorption peaks at 565 $cm^{-1}$.

**c=** distance from the baseline to the lowest point between **a** and **b**.

#### 2.2.6. Change of color

The measurement of color change is one of the most important properties of archaeological bones. It shows the current state of preservation or deterioration of archaeological bones. Color changes of the samples studied were measured using the CIE*Lab system. The L* scale measures lightness, and

varies from 0 (black) to 100 (perfect white). The a* scale measures red-green; +a means more red, -a means more green. The b-scale measures yellow- $\Delta E = \sqrt{(\Delta L)^2 + (\Delta a)^2 + (\Delta b)^2}$ yellow, -b more blue. Differences in color between two specimens are determined by the use of the Greek letter Delta (L, a, b) The total color difference (ΔE) is found according to the following equation:

The measurement was made using a portable spectrophotometer by Hunter Lab-Reston Virginia USA.

#### 2.2.7. Contact angle measurement (wettability)

The contact angle of samples were tested. This test was done using Compact Video Microscope (CVM) manufactured by SDL- UK. The average water drop volume applied to the surface of the tested samples was 250 µL this test was carried out under environmental conditions at a temperature of 22±1ºC and relative humidity of 65±5%. The expanded measurement uncertainty was ±1º (coverage factor, k=2 for a confidence level of 95%) [27].

#### 2.2.8. Isolation and identification of fungi

##### 2.2.8.1. *Fungal isolation*

Deteriorated archaeological bones were used for the isolation of fungi. The deteriorated bone parts were suspended in sterile distilled water and shake well on a reciprocal shaker for 2h and left to stand for 10 min then the filtrates were serially diluted up to $10^{-3}$ and 200µl from each dilution were used to inoculate potato dextrose Petri dishes (15cm diameter) supplemented with neomycin (50mg/L) as antibacterial and Rose Bengal (30mg/L) to prevent fungal overgrowth [34]. The dishes were sealed with parafilm and incubated at 27°C for 3-6 days, and growth was observed after two days. The incubation period for each fungus was recorded. This was taken when the first visual growth was observed from the plating date and considered an incubation period of growth [35].

##### 2.2.8.2. *Fungal identification*

The isolated fungal strains were taxonomically identified depending on their morphological characteristics according to identification keys using specific media; Czapek Agar for *Aspergillus* [36-39]. Czapek yeast extract Agar, potato dextrose agar, and malt extract agar were used for the identification of miscellaneous fungi and other ascomycetes [20,26, 38,39].

## 3. Results

### 3.1. *Photographic documentation (visual assessment)*

It was clear from the visual assessment that the cow's cranium was completely covered with dust and particulates, fig. (1-a). The frontal and nasal bones were broken and detached. These fractures were postmortem and probably caused by post depositional environments. The cow's cranium was fixed on the wooden plate using thick iron holders, which contacted the outer layer of the bone and caused some corrosion. The data obtained, fig. (1-b & c) showed the cow's horn on both sides is full of dirt, and a large part of it is broken. The data, fig. (1-d) showed the broken part in the front of the cow's cranium with some insect bores and some cracks. The data, fig. (1-e) showed a part of the eye with some fine cracks, erosion on the edges of the eye, and the accumulation of dust and dirt from inside and outside the eye. The data obtained, fig. (1-f & j) showed some aspects of deterioration appeared on the back side of the cranium such as change of color, cracks, erosion, accumulated dust, and dirt, missed parts, and insect bores.


**Figure (1)** photographic documentation of the cranium; **a.** general photo of the cranium studied, **b., c.** both sides of cow's horn, **d., e.** the broken front part of the cranium, **f.-J.** different dete-rioration aspects of the behind the side of the cranium.

### 3.2. *Digital light microscope*

It was clear from the data obtained, fig. (2-a) that the surface of the Bos taurus cranium is smooth, and its color is approx. white. Very fine white dots appear, and there are also some fine black dots around them. By investigating different places of the archaeological cranium, the following aspects of deterioration was found: **a)** color change, fig. (2-b & h)**:** The color of the cranium has changed from the normal color of the bones after death (which tends to be white). The color of the bone ranged from light cream to dark brown and appeared gray in some places. **b)** bioerosion, the results showed the presence of bioerosion on the surface of the cranium, fig. (2-c & f). The results showed small channels and microscopic focal destruction. **c)** cracks: The results showed very thin transverse cracks, fig. (2-d). pitting, the results showed some pitting on cranium vault, fig. (2-e, f & h).

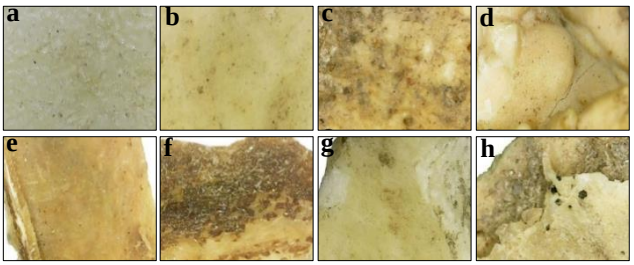


**Figure (2)** digital light microscope investigation of different parts of the studied cranium

### 3.3. *SEM morphological features*

The results showed no significant change in the surface morphology and texture of the modern cranium, fig. (3-a). The surface was smooth, and haversian canal was easily recognized. Also, the pores of the bone remained open without any visible clogging. For archaeological cranium, fig. (3-b-d), some aspects of deterioration were found on the surface of the bones. One of the most important aspects of deterioration is the lack of the Haversian canal in all samples and the presence of cracks of different sizes and shapes. It was observed that the surface was uneven, and the presence of abrasion on the samples' surfaces led to the loss of the characteristic features of the bone surface. A degree of erosion was also apparent. It was also observed that some signs of microbial infection may be from fungi or bacteria. This was proven through fungal examination, and the presence of some decomposing fungi.

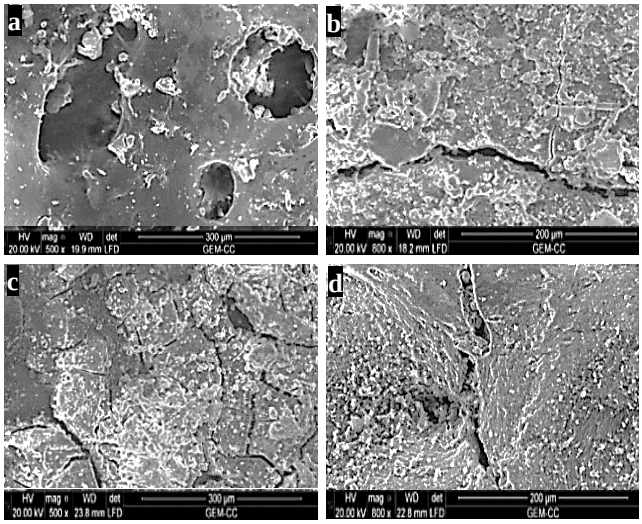


**Figure (3)** SEM photomicrographs of the samples surface morphology **a.** new sample, **b.**, **c.**, **d.** archaeological bone samples.

### 3.4. *Polarized light microscope*

It was clear from the data obtained from the new sample, fig. (4-a & b) that the small dark dots are lacunae that once held bone cells. The big dark dots in plain and polarized light refers to Haversian systems. The Long black streaks show the banded pattern of collagen in bone. It was clear from the new bone sample that it comes densely packed with collagen, which appeared bright yellowish golden under plain and polarized light. The archaeological samples under plain and polarized light, fig. (4-c & d) showed traces or no collagen fibers since the color varied from dark brown to black colors, which indicated the degradation of the bone surface during the burial environment or after long exposure to improper conditions in excavation or in the museum. It was also clear that the characteristic details of the bone surface such as lacunae or Haversian systems cannot be recognized compared to the new bone sample. It was also noticed focal destruction and loss of birefringence as a result of taphonomic alterations caused by microbial destruction, weathering, mineral replacement, protein degradation, etc.

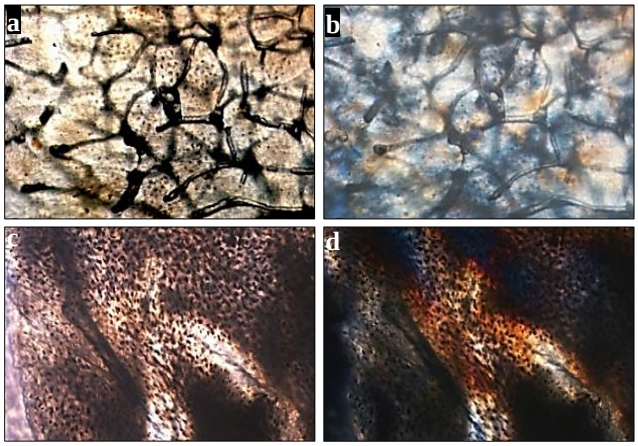


**Figure (4)** PLM of new and archaeological bone samples; **a.**, **b.** new sample under plain light (100-X) and polarized light (100-X) respectively; **c.**, **d.** archaeological sample under plain light (100-X) and polarized light (100-X) respectively.

### 3.5. *ATR/FTIR results of new and archaeological bones*

It is known that bone consists of the organic and inorganic compounds. For organic phase in new and archaeological bone samples, amide groups appeared at different wave-numbers. It was clear from the obtained data, fig. (5) that the amide A appeared at the wavenumber of 3313.60 $cm^{-1}$, and 3266.74 with intensities of 0.0005 and 0.0062 for new and archaeological samples respectively. This band is assigned to a broad band that represents (OH) hydroxyl stretching due to the intermolecular hydrogen bonding of the hydroxyl group [29]. It also refers to the NH group as diversely hydrogen-bonded [40]. The amide B wavenumber appeared at 2350.61 $cm^{-1}$, and 2349.19 $cm^{-1}$ with intensities of 0.008 and 0.014 for the new and archaeological samples respectively. This band is associated with the stretching of peptide N-H groups involved in inter-chain hydrogen bonding. The amide I appeared at 1648.21 $cm^{-1}$ and with an intensity of 0.005. This band shifted to a low wavenumber for an archaeological sample and appeared at 163086 $cm^{-1}$ with intensity 0.017, which was considered high compared to the new sample. The amide I band is primarily caused by the stretching vibrations of the peptide carbonyl group (C=O) coupled weakly with C-N stretching and N-H bending. It is sensitive to local order and its exact position is deter-mined by the backbone conformation and the hydrogen-bonding pattern within the protein molecule [41]. Amide II appeared at 1544.56 $cm^{-1}$ and at 1541.48 $cm^{-1}$ with intensities 0.003 and 0.016 for the new and archaeological samples respectively. This band is mainly derived from the C-N stretch along with N-H in-plane bending. It is sensitive to conformational changes, too. For the inorganic phase, The FTIR spectra of the bio-apatite bone fraction are rep-resented by vibration bands of mainly $CO_3$ and $PO_4$. The vibrational peaks for the phosphate group appeared approx. at 565, 605, and 1035 $cm^{-1}$ for new and archaeological samples respectively. The vibrational peaks for the carbonate group appeared approximately at 710, 874, and 1415 $cm^{-1}$ for the new and archaeological samples respectively [33]. The intensities of

the peaks of phosphate and carbonate for archaeological samples increased compared to the new one, which indicated the chemical changes and deterioration. The data showed that the carbonate/phosphate (C/P) content calculation of the new bone sample was 0.44, and for the archaeological sample was 0.60. The data also showed that the crystallinity index was 2.72 for the new bone sample and 4.30 for the archaeological sample.

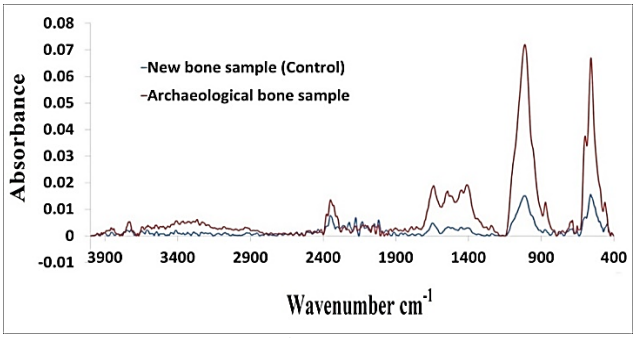


**Figure (5)** ATR/FTIR analysis of new and archaeological bone samples.

### 3.6. *Change of color*

It was clear from the data obtained, tab. (1) that the lightness (L* value) of the new bone sample recorded was 88.13. The L* value of the archaeological samples taken from different assessment sites was between 62.10 and 35.71, with a percentage loss between 30% and 59%. For the red-green color (a* value), all results stated that the color tends to be red color. The lowest value of the red color was obtained from the new bone sample. The highest value of red color was obtained from the archaeological sample site No. 4. The red color ranged between 2.30 for the new sample, and 55.10 for the sample site No, 4. The color of the b* value tends to be yellow. The yellow color increased with color measurements taken from different places of the archaeological cranium The lowest yellow color was obtained from the new sample (3.5). The highest yellow color was obtained from a measurement taken from the sample site No. 2. The total color difference (ΔE) indicated that there was a high change in all measurement taken from the archaeological bone.

**Table (1)** Change of color of new and archaeological samples taken from different sites of the cranium

| Samples | Color values | | | (ΔE) |
|---|---|---|---|---|
| | *L** | *a** | *b** | |
| New sample | 88.13 | 2.30 | 3.50 | **0.00** |
| Arch. sample (site 1) | 62.10 | 12.39 | 44.20 | **49.40** |
| Arch. sample (site 2) | 60.09 | 25.20 | 32.45 | **46.40** |
| Arch. sample (site 3) | 55.76 | 34.90 | 23.50 | **50.10** |
| Arch. sample (site 4) | 50.55 | 55.10 | 29.29 | **69.80** |
| Arch. sample (site 5) | 40.12 | 7.31 | 9.15 | **48.60** |
| Arch. sample (site 6) | 35.71 | 5.89 | 7.32 | **52.70** |

### 3.7. *Contact angle of new and arch. bones*

Figure. (6) showed that the contact angle of the new bone sample was 76°, while it was 44° in the archaeological bone sample, where the loss rate was 42%. It is well known that bone is considered a porous material [42]. Therefore, the value of the contact angle in the new bone sample is considered normal. The contact angle of the archaeological bone sample is considered low.

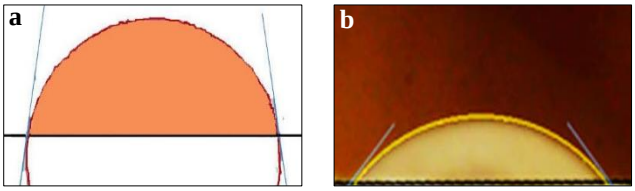


**Figure (6)** contact angle of **a.** new sample (70°), **b.** arch. bone sample (44°).

### 3.8. *Isolation and identification of fungi*

The isolated four fungal strains from the archaeological cranium studied were subjected to taxonomical identification based on morphological features. According to the used keys, the four fungi identified were *Penicillium chrysogenum*, *Aspergillus niger*, *Aspergillus terreus*, and *Cladosporium cladosporioides*, fig. (7).

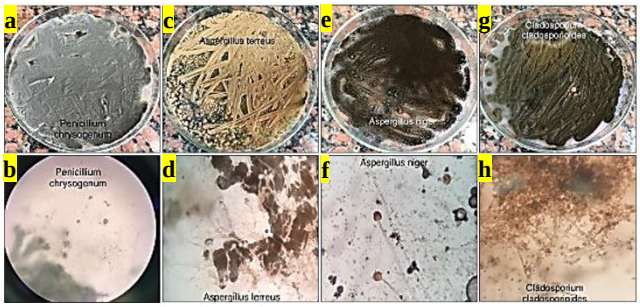


**Figure (7)** identified fungi from the arch. cranium; **a.**, **b.** *Penicillium chrysogenum*, **c.**, **d.** *Aspergillus terreus*, **e.**, **f.** *Aspergillus niger*, **g.**, **h.** *Cladosporium cladosporioides.*

## 4. Discussion

Photographic documentation (visual assessment) showed some cracks in the front of the cow's cranium. The cracks may be attributed to the fluctuation in relative humidity and temperature either in the burial environment or in the museum [5]. The investigation of the studied cranium by digital light microscope showed some aspects of deterioration. One of these aspects was the change of color. **a)** The change in the color of the cranium may be due to one or more of the following reasons: Some metals (such as manganese, zinc, iron, etc.) can be incorporated in bone through sorption from the soil solution, or by intake during life [43]. Cream and brown colors may be caused by staining from anaerobic peat bog conditions, although a variety of colors can arise from different surrounding deposits [44]. Gray and white colors were also noticed, fig. (2-c). The white color may be resulted from burning at extremely high temperatures, such as the temperature needed for cremation [44]. Weathering processes could cause color changes on the bone surface [45]. The color change somet-imes results from the effect of some microorganisms, fig. (2-c, f, g & h) such as fungi or bacteria, which produce acids or enzymes that interact with bone components and produce pigments or dyes that distort the bone surface [46]. **b)** Bioerosion such as small channels and microscopic focal destruction was

also noticed on the surface of the cranium. Bioerosion or biogenic bone degradation refers to destruction or restructuring, and the abrasion of hard substrates of bone microanatomy by microorganisms, such as bacteria and fungi [47]. This was confirmed by the identification of some decomposing fungi, as will be explained in another section of the study. Végh, et al. [48] reported that morphological changes to bone resulting from bioerosion include microscopic focal destruction which can be linear longitudinal, lamellate, or budded, small channels caused by fungi, and other types of diagenetic changes, such as inclusions, redu-ction in birefringence, and infiltrations. **c)** Thin cracks were also found on the cranium. There are some causes for cracks in archaeological bones. Tappen and Peske [49] reported that cracks in the bone resulting from post-mortem weathering and shrinkage are oriented in basically the same direction as those produced by split-line patterns made after decalcification. Abdel-Maksoud and Abdel-Hady [44] stated that cracks may be result from the conditions of archaeological bones after excavation, which can cause a minor way to development of cracks. It seems possible that these cracks may be related to stresses caused by bone expansion and contraction whilst buried. They also reported that fluctuations in soil moisture and temperature are significant in the destruction of bone. Pokines, et al. [50] explained that Crack propagation often parallels the osteon structure, following the weaker planes in the bone, and cracking may be enhanced by thermal expansion contraction from daily sun exposure. Cracking also is caused in part by freeze-thaw cycles, where expanding ice crystals force the bone apart and form cracks. **d)** Some pitting were also found on the cranium. The causes of pitting in the archaeological bones are due to some factors, including the presence of salts, especially soluble salts such as sodium chloride, which crystallizes on the surface after the water, evaporates, dissolved again with increasing water, and then crystallizes, and this leads to pitting. Also, the presence of sand and gravel, along with the presence of water sources in the burial environment, creates friction on the bone surface and leads to pitting on the surface of the bones [44,51]. The investigation of the cranium by a SEM showed some aspects of deterioration such as a lack of the Haversian canal, cracks, erosion, and some signs of microbial infection. These aspects were due to physical, chemical, and biological factors either in the burial environment or in museum condition. The investigation of the cranium by polarized light microscope showed that the surface of archaeological sample suffered from degradation which was due to taphonomic alterations, while the new bone sample (control) showed all the characteristic details of the mineralized collagen fibril bundles. It was clear from FTIR analysis that the amide groups (amide A, amide B, amide I, and amide II) of archaeological samples shifted to lower values with high intensities compared to the new sample, which indicate chemical changes and deterioration. For inorganic phase, the increasing of the peaks intensities of phosphate and carbonate, and high crystallinity index of the archaeological sample compared to the new bone sample may be attributed to the chemical changes occurring in the archaeological samples, which may have resulted from the burial environment's influence. The results of the color values (L*, a*, and b*) showed that yellow, brown, and gray colors were found on the surface of the studied cow's cranium. The variation of colors was due to the effect of individual or combination factors derived from the effect of surrounding environmental condition or from human factor related deterioration such as improper handling. The yellow and brown colors may be due to contact with soils, and water, or may be dirty from handling [52]. Argáez, et al. [53] stated that the primary cause of red and yellow pigmentation is from ocher, a clay-like soil that when combined with water can make a non-toxic oil-like paint. When found at burial sites it is primarily assumed that the deceased individual's skin was covered in red ochre as part of the funerary rituals. The observable changes in surface color may be regarded as an outward reflection of the modification of the chemical composition of bone in the presence of heat [5]. The reduction in the contact angle of the archaeological bone sample may be due to the increased porosity of the bone. The porosity of archaeological bones can increase for many reasons [54]. One of these reasons is skeletal diseases, which can rapidly form woven bone that is poorly organized and always has a porous appearance due to the loose organization of the mineralized osteoid fibers, and tends to contain more vascular spaces than compact bone. Bone porosity can be also due to the individual response (according to sex, age, and immune reaction), to taphonomy (interaction of bone with soil, degradation), and to different Pathological conditions such as anemia, treponematosis, or osteoporosis [55]. It can also be said that taphonomic degradation resulting from multiple factors in the burial environment (for example, the effect of water, salts, low pH value, etc.) plays a major role in increasing bone porosity, and makes it a hydrophilic material. Accordingly, some or all factors mentioned above play a major role in the reduction of the contact angle of the archaeological bone sample. Some fungi were isolated and identified from the studied cranium. Elserogy et al. [56] isolated *Penicillium chrysogenum* from bones and related materials. All the isolated fungi have the ability to produce proteases enzymes which play an important role in the deterioration of archaeological bones and other organic materials [57-62].

## 5. Conservation Methods

As a result of the various aspects of deterioration found on the cranium, the conservation treatments used included the following steps:

### 5.1. *Cleaning*

Cleaning is considered one of the vital processes in cleaning archaeological bones from dust, dirt, and stains from various sources. The cleaning process included two steps. The first step started with mechanical cleaning. Conservators always begin with mechanical cleaning as it is a widespread and applicable process, a method that is safe for the archaeological material and for the conservator, and is

inexpensive. It is also a non-toxic and residue-free process which counts as another advantage [28,63]. Mech-anical cleaning was performed with different devices, fig. (8-a & b). Very soft brushes of different sizes were used to remove loose dust from the surface of the cranium and in other narrow openings such as the ear, etc. Some dental tools and blunt scalpels were used very carefully (so as not to scratch the surface of the bone) in some narrow openings to remove some hard dust. It should be noticed that the hard dust was removed under control using a magnifying glass. An electric blower with low pressure was also used to remove loose dust between narrow openings. Wet cleaning using water was used to remove hard dust that mechanical cleaning could not remove. Wet cleaning was done using a cotton swab soaked in distilled water. It can be said that this method was highly efficient in removing some dust. Wet cleaning has the advantage of being readily available, low-cost, and non-toxic [63]. Chemical cleaning, fig. (8-c) using isopropyl alcohol was also applied to remove the remains of dust after mechanical and wet cleaning. It is important after wet cleaning to remove the remains of water from bone artifacts in order to prevent the effect of water on the bones and to prevent any chance of microbial infec-tions as a result of using water for wet cleaning. The use of isopropyl alcohol solution was applied with cotton buds, which gives a more controlled cleaning with less risk to the surface and to the highly hygroscopic organic material like bone [64]. The use of isopropyl alcohol also plays an important role in inhibiting microbial growth, although its effect is only at work time and not in the long term. A mixture of isopropyl alcohol and water was also used to remove some dark stains from the surface of the bone.

### 5.2. *Consolidation*

Due to the presence of some parts of the cranium in a weak condition, it was necessary to use one of the consoli-dants (which was evaluated in a previous study and proved successful) in the consolidation of the cranium in general, fig. (8-d). Sodium alginate was used for this purpose. Sodium alginate is a linear unbranched, amorphous copolymer usually extracted from various seaweeds and composed of -D-man-nuronic acid (M) and -L- guluronic acid (G) linked by 1.4 glycosidic bonds [65]. Sodium alginate was used because it has become an important family of polysaccharides with a wide range of applications and uses in different fields such as gelling, film-forming ability, non-toxic, biocompatibility, ionic crosslinking, processability, and biodegradability. It was generally stable to extended periods of light exposure, and had little effect on acidity, and color change[5]. Sodium alginate was applied at a concentration of 1.5% by spray method. The cranium was left to dry naturally at room temperature (21 $^{o}$C ± 2 $^{o}$C).

### 5.3. *Disinfection*

Disinfection of bone, fig. (8-d) is a necessary process to ensure microbial inhibition at the time of conservation treatment, and to give future protection against any microbial contamination. As a result of the isolation of some decomp-osing fungi from the studied cranium, it was necessary to use disinfection protocol for the cranium. Silver nanoparticle (Ag-NPs) was used for this purpose. It was selected because of its optical proper, surface charge, size, shape, and electrical conductivity make it a promising nanostructure for various applications such as photocatalysts, and bios-ensors, besides their antifungal, antiviral, antibacterial, and antioxidant activity [29]. Silver nanoparticles were applied at a concentration of 300 ppm by spray method.

### 5.4. *Exhibition of the cranium*

#### 5.4.1. Display the cranium on a Plexiglas base

The cranium was fixed with non-isolated metal screws on a wooden base, and the metal screws affected the bones in the places where they touched, fig. (8-e). Accordingly, the non-insolated metal screws were removed and the wooden base was replaced with another made of Plexiglas. The cranium was installed on a base of Plexiglas 40×50 with a thickness of 8 mm to maintain the balance of the cranium, fig. (8-f). It was also supported using straps of Plexiglas with a thickness of 5 cm. These strips were used as bonds for the cranium in order to maintain its balance during display and prevent it from moving when vibrating, with fixing of the straps to the base by Paraloid B. 72 (ethyl methacrylate/ methyl acrylate copolymer). Plexiglas is a polymer of methyl methacrylate. Its specific density is 1.19. It was selected for some reasons including its transparency, since it is similar to the clarity of crystal; the rate of light trans-mission is 93%, it has good durability and does not yellow or change over time. Plexiglas can be bent and formed and bear large weights. The thicker types are of high hardness, resistant to climatic effects, and can tolerate temperatures from zero to 160 degrees Celsius. It is not subject to interaction with inorganic substances and hydrocarbons. It is corrosion and shock resistant. It is resistant to most chemicals.

#### 5.4.2. Recommendation for exhibition of the cranium

It was recommended to the museum's management team that the new Plexiglas base on which the cranium was attached should be placed inside a controlled showcase. Provided that the relative humidity levels are 50% ± 5%, the temperature is 20±2 $^{o}$C, and the light intensity does not exceed 50 Lux/hour, with filters for ultraviolet radiation, and the presence of filters to absorb pollutants, dust, and particulates.

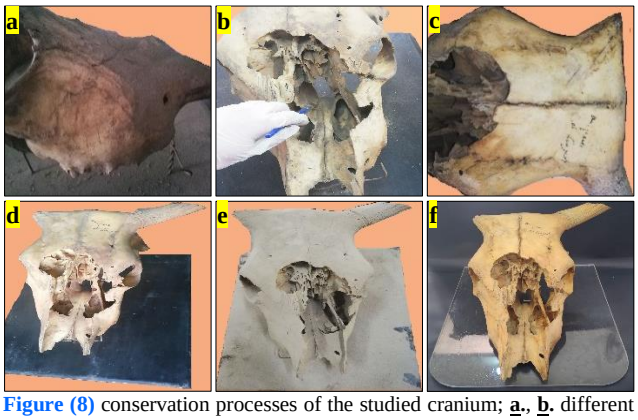


**Figure (8)** conservation processes of the studied cranium; **a.**, **b.** different steps of mechanical cleaning, **c.** chemical cleaning, **d.** after consolidation and disinfection processes, **e.** before conserve-ation, **f.** after finishing conservation and display on Plexiglas stand.

## 6. Conclusion

*The current study proved that the archaeological cranium sample suffered from severe deterioration. Various aspects of deterioration were noticed, such as discoloration, bioerosion, pitting, cracks, etc. All analyses and investigation techniques used proved that all aspects of deterioration were due to physical, chemical, and biological deterioration factors that affected changes in the properties of the studied cranium bones. Digital, SEM, and polarized microscopes showed cracks, pitting, stains derived from different sources, and loss of bone surface characteristics such as the absence of haversian systems, lacunae, etc. The FTIR analysis also demonstrated the presence of chemical changes in the cranium, as the wavenumbers of the cranium bone shifted to lower values and intensities were high compared to the control sample. The crystallinity index of archaeological samples was also increased than the new sample. High change in the color value and total color differences of the cranium compared to the new sample. The contact angle of the archaeological cranium was much less than the control sample. This indicated that the porosity of the archaeological bone cranium was higher than the control sample. This may be due to some factors including diseases, and taphonomic degradation in the burial environment resulting from several factors such as water content, salts, low pH, etc., which make it a hydrophilic material. The most occurrence fungi were Penicillium chrysogenum, Aspergillus niger, Aspergillus terreus, and Cladosporium cladosporioides. Some references mentioned in the results and discussion section above produce enzymes that, in turn, interact chemically with the bones and lead to their deterioration. Accordingly, the conservation treatment process became vital and necessary to stop the interaction of various deterioration factors, or to reduce them. The major conservation processes included cleaning, consolidation, and disinfection. Finally, the cranium was displayed on a Plexiglas stand instead of the old wooden stand. Effective assessment of the bone condition helped to improve the conservation outcome drastically, despite the promising results of the conservation of the studied sample; yet the authors recommend applying such techniques and conser-vation methods to a more large and diverse osteological collections.*


## Acknowledgments

The authors extend their sincere thanks, appreciation, and gratitude to the management staff of the Agricultural Museum in Giza, Egypt for providing all administrative assistance during the conduct of this research.


## References


**[1]** Legan, L., Leskovar, T., Črešnar, M., et al. (2020). Non-invasive reflection FTIR characterization of archaeological burnt bones: Reference database and case studies. *J. of Cultural Heritage*. 41: 13-26.

**[2]** Abdel-Maksoud, G. & El-Sayed, A. (2016). Analysis of archaeological bones from different sites in Egypt by a multiple technique (XRD, EDX, FTIR). *MAA*. 16: 149-158.

**[3]** Abdel-Maksoud, G., El-Sayed, A. (2016). Microscopic investigation for condition assessment of archaeological bones from different sites in Egypt. *IJCS*. 7: 381-394.

**[4]** El-Naggar, M., Gaballah, S., Abdel-Maksoud, G., et al. (2022). Preparation of bactericidal zinc oxide nanoparticles loaded carboxymethyl cellulose/polyethylene glycol cryogel for gap filling of archaeological bones. *J. of Materials Research and Technology*. 20: 114-127.

**[5]** Abdel-Maksoud, G., Gaballah, S., Youssef, A.M., et al. (2023). Eco-friendly approach for control of fungal deterioration of archaeological skeleton dated back to the Greco-Roman period. *J. of Cultural Heritage*. 59: 38-48.

**[6]** Matthiesen, H., Eriksen, A., Hollesen, J., et al. (2021) Bone degradation at five Arctic archaeological sites: Quantifying the importance of burial environment and bone characteristics. *J. of Archaeological Science*. 125: 1-9.

**[7]** Child, A. (1995). Microbial taphonomy of archaeological bone. ***Studies in Conservation***. 40: 19-30.

**[8]** Baxter, K. (2004). Extrinsic factors that effect the preservation of bone. *The Nebraska Anthropologist*. 19: 38-45.

**[9]** Manifold, B. (2012). Intrinsic and extrinsic factors involved in the preservation of non-adult skeletal remains in archaeology and forensic science. *Bulletin of the International Association for Paleodontology*. 6: 1-19.

**[10]** Guy, H., Masset, C. & Baud, C. (1997). Infant taphonomy. *Int. J. of Osteoarchaeology*. 7: 221-229.

**[11]** Morton, R. & Lord, W. (2006). Taphonomy of child-sized remains: A study of scattering and scavenging in Virginia, USA. *J. of Forensic Sciences*. 51: 475-479.

**[12]** Von Endt, D., & Ortner, D. (1984). Experiment effects of bone size and temperature on bone diagenesis. *J. of Archaeological Science*. 11: 247-253.

**[13]** Breitmeier, D., Graefe-Kirci, U., Albrecht, K., et al. (2005). Evaluation of the correlation between time corpses spent in in-ground graves and findings at Exhumation. *Forensic Science Int*. 154: 218-223.

**[14]** Hanson, D. & Buikstra, J. (1987). Histomorphological alteration in buried human bone from the lower Illinois Valley: implications for palaeodietary research. *J. of Archaeological Science*. 14: 549-563.

**[15]** Wittmers, W., Aufderheide, A., Pounds, J., et al. (2008). Problems in determination of skeletal lead burden in archaeological samples: An example from the first African baptism church population. *Am. J. of Physical Anthropology*. 136: 379-386.

**[16]** Hedges, J. & Millard, A. (1995). Bones and groundwater: Towards the modelling of diagenetic processes. *J. of Archaeological Science*. 22: 155-164.

**[17]** Hedges, R., Millard, A. & Pike, A. (1995). Measurements and relationships of diagenetic alternations of bone from three archaeological sites. *J. of Archaeological Science*. 22: 201-209.

**[18]** Nicholson, R. (1996). Bone degradation, burial medium and species representation: Debunking the myths, an experiment-based approach. *J. of Archaeological Science*. 23: 513-533.

**[19]** Locock, M., Currie, C. & Gray, S. (1992). Chemical changes in buried animal bone: Data from a postmedieval assemblages. *Int. J. of Osteoarchaeology*. 2: 297-304.

**[20]** Gaballah, S., El-Nagar, M., Abdel-Maksoud, G., et al. (2021). Presenting shape memory polymers SMP and some reinforcement materials for gaps filling in archaeological bones. *Egyptian J. of Chemistry*. 64: 3605-3614.

**[21]** Nielsen-Marsh, C., Smith, C., Jans, M., et al. (2007). Bone diagenesis in the European Holocene II: taphonomic and environmental considerations. *J. of Archaeological Science*. 34: 1523-1531.

**[22]** Abdel-Maksoud, G. (2011). Investigation techniques and conservation methods for a historical parchment document. *J. of the Society of Leather Technologists and Chemists*. 95: 23-34.

**[23]** Abdel-Maksoud, G., Al-Shazly, E. & El-Amin, A. (2011). Damage caused by insects during mummification process: An experimental study. *Archaeological and Anthropological Sciences*. 3: 291-308.

**[24]** Fouda, A., Abdel-Nasser, M., Khalil, A., et al. (2022). Investigate the role of fungal communities associated with a historical manuscript from the 17th century in biodegradation. *NPJ Materials Degradation*. 88: 1-13.

**[25]** Abdel-Maksoud, G. & El-Amin, A. (2013). The investigation and conservation of a gazelle mummy from the late period in ancient Egypt. *MAA*. 13: 45-67.

**[26]** Abdel-Maksoud, G. (2010). Comparison between the properties of "accelerated-aged" bones and archaeological bones. *MAA*. 10: 89-112.

**[27]** Abdel-Maksoud, G., Awad, H., Rashed, U., et al. (2022). Preliminary study for the evaluation of a pulsed coaxial plasma gun for removal of iron rust stain from bone artifacts. *J. of Cultural Heritage.* 55: 128-137.

**[28]** Abdel-Maksoud, G., Hussien, N. M., Al-Arif, N., et al. (2022). Evaluation of a Mixture of Castor Oil and Polyvinylpyrrolidone for the Lubrication of Dry Vegetable Tanned leather artifacts. *J. of the Society of Leather Technologists and Chemists*. 106: 20-31.

**[29]** Abdel-Maksoud, G., Ghozy, H., Ezzat, R., et al. (2023). Evaluation of the efficiency of sodium alginate for the consolidation of archeological bones. *Egyptian J. of Chemistry*. 66: 357 – 366.

**[30]** Dal Sasso, G., Asscher, Y., Angelini, I., et al. (2018). A universal curve of apatite crystallinity for the assessment of bone integrity and preservation. *Scientific Reports*. 8: 1-13.

**[31]** Weiner, S. & Bar-Yosef, O. (1990). States of preservation of bones from prehistoric sites in the Near East: A survey. *J. of Archaeological Science*. 17: 187-196.

**[32]** Stiner, M., Kuhn, S., Weiner, S., et al. (1995). Differential burning, recrystallization, and fragmentation of archaeological bone. *J. of Archaeological Science*. 22: 223-237.

**[33]** Thompson, T., Gauthier, M. & Islam, M. (2009). The application of a new method of Fourier Transform Infrared Spectroscopy to the analysis of burned bone. *J. of Archaeological Science*. 36: 910-914.

**[34]** Martin, J. (1950). Use of acid, rose Bengal, and streptomycin in the plate method for estimating soil fungi. *Soil Science*. 69: 215-232.

**[35]** Abdel-Aziz, M. & Hezma, A. (2013). Spectroscopic and antibacterial evaluation of nano-hydroxapatite polyvinyl alcohol biocomposite doped with microbial-synthesized nanogold for biomedical applications. *Polymer-Plastics Technology and Engineering*. 52: 1503-1509.

**[36]** Raper, K. & Fennell, D. (1965). *The genus aspergillus*, Williams & Wilkins, Baltimore.

**[37]** Klich, M. (2002). *Identification of common Aspergillus species*. Amer Society for Microbiology, USA.

**[38]** Von Arx, J. (1970). *The genera of fungi sporulating in pure culture*, Verlag Von J. Cramer, Germany.

**[39]** Watanabe, T. (2002). *Pictorial atlas of soil and seed fungi: Morphologies of Cultured Fungi and Key to Species*, CRC Press, Boca Raton.

**[40]** Saada, N., Abdel-Maksoud, G., Abd El-Aziz, M. S., et al. (2021). Green synthesis of silver nanoparticles, characterization, and use for sustainable preservation of historical parchment against microbial biodegradation. *Biocatalysis and Agricultural Biotechnology*. 32, doi: 10.1016/j.bcab.2021.101948.

**[41]** Sebestyén, Z., Badea, E., Carsote, C., et al. (2022). Characterization of historical leather bookbindings by various thermal methods (TG/MS, Py-GC/MS, and micro-DSC) and FTIR-ATR spectroscopy. *J. of Analytical and Applied Pyrolysis*. 162: 1-12.

**[42]** Johnson, J. (1998). Soluble salts and deterioration of archeological materials. *Conserve O Gram*. 6 (5): 1-4.

**[43]** Opez-Costas, O., Lantes-Suarez, O. & Cortizas, A. (2016). Chemical compositional changes in archaeological human bones due to diagenesis: Type of bone vs soil environment. *J. of Archaeological Science*. 67: 43-51.

**[44]** Abdel-Maksoud, G., Abdel-Hady, M. (2011) Effect of burial environment on crocodile bones from Hawara excavation, Fayoum, Egypt, *J. of Cultural Heritage*. 12: 180-189.

**[45]** Koon, G., Nicholson, R. & Collins, M. (2003). A practical approach to the identification of low temperature heated bone using TEM, *J. of Archaeological Science*. 30: 1393-1399.

**[46]** Cole, G. & Waldron, T. (2016). Purple staining of archaeological human bone: An investigation of probable cause and implications for other tissues and artifacts. *J. of Anthropology*. 2016 (2): 1-11.

**[47]** Davis, P. (1997). The bioerosion of bird bones. ***Int. J. of Osteoarchaeology***. 7: 388-401.

**[48]** Végh, E., Czermak, A., Márquez-Grant, N., et al. (2021). Assessing the reliability of microbial bioerosion features in burnt bones: A novel approach using feature-labelling in histotaphonomical analysis. *J. of Archaeological Science*. 37, doi: 10.1016/j.jasrep.2021.102906.

**[49]** Tappen, N. & Peske, G. (1970). Weathering cracks and split-line patterns in archaeological bone. *American Antiquity*. 35: 383-386.

**[50]** Pokines, J., Faillace, K., Berger, J., et al. (2018). The effects of repeated wet-dry cycles as a component of bone weathering. *J. of Archaeological Science Reports*. 17: 433-441.

**[51]** Frontini, R., Fernández-Jalvo, Y., Fernández, M., et al. (2019). Abrasion in archaeological fish bones from sand dunes. An experimental approach. *Archaeological and Anthropological Sciences*. 11: 4891-4907.

**[52]** Dupras, T. & Schultz, J. (2021). Taphonomic bone staining and color changes in forensic contexts. In: Pokines, J., L'Abbé, E., Symes, S. & (eds.) *Manual of Forensic Taphonomy*, Ch. 12, CRC Press, Boca Raton, pp. 315-340.

**[53]** Argáez, C., Batta, E., Mansilla, J., et al. (2011). The origin of black pigmentation in a sample of Mexican prehispanic human bones. *J. of Archaeological Science*. 38: 2979-2988.

**[54]** Devlin, J. & Herrmann, N. (2008). Bone color as an interpretive tool of the depositional history of archaeological cremains. In: Schmidt, Ch. & Symes, S. (eds.) *The Analysis of Burned Human Remains*, Schmidt, Ch. & Symes, S., Ch. 6, Elsevier, Amsterdam, pp. 109-128.

**[55]** Mansilla, J., Moreno-Castilla, C., Bosch, P., et al. (2014). On porosity of archeological bones II. Textural characterization of Mesoamerican human bones. *Palaeogeography, Palaeoclimatology, Palaeoecology*. 414: 493-499.

**[56]** Elserogy, A., Kanan, G., Hussein, E., et al. (2016). Isolation, characterization and treatment of microbial agents responsible for the deterioration of archaeological objects in three Jordanian museums. *MAA*. 16: 117-126.

**[57]** Haq, I., Mukhtar, H. & Umber, H. (2006). Production of protease by penicillium chrysogenum through optimization of environmental conditions. *J. of Agriculture and Social Sciences*. 2: 23-25.

**[58]** Osman, M., Khattab, O. & Elsaba, Y. (2014). Aspergillus terreus proteases: Characterization and applications. *J. of Chemical, Biological and Physical Sciences*. 3: 2333-2346.

**[59]** Racheal, O., Ahmed, A., Ndigwe, E., et al. (2015). Extraction, purification and characterization of protease from aspergillus niger isolated from yam peels. *Int. J. of Nutrition and Food Sciences*. 4 (2): 125-131.

**[60]** Abdel-Nasser, M., Abdel-Maksoud, G., Eid, A., et al. (2023). Antifungal activity of cell-free filtrate of probiotic bacteria Lactobacillus rhamnosus ATCC-7469 against fungal strains isolated from a historical manuscript. *Microorganisms*. 11 (5), doi: 10.3390/microorganisms11051104.

**[61]** Fouda, A., Abdel-Nasser, M., Eid, A., et al. (2023). An eco-friendly approach utilizing green synthesized titanium dioxide nanoparticles for leather conservation against a fungal strain, penicillium expansum AL1, involved in the biodeterioration of a historical manuscript. *Biology*, Vol. 12 (1025): 1-26.

**[62]** Abdel-Maksoud, G., Abdel-Nasser, M. & Hassan, S. (2023). Biosynthesis of titanium dioxide nanoparticles using probiotic bacterial strain, lactobacillus rhamno-sus, and evaluate of their biocompatibility and antifungal activity. *Biomass Conversion and Biorefnery*, doi: 10.1007/s13399-023-04587-x

**[63]** López-Polín, L. (2012). Possible interferences of some conservation treatments with subsequent studies on fossil bones: A conservator's overview. *Quaternary Int*. 275: 120-127.

**[64]** Abdel-Maksoud, G., Emam, H. & Ragab, N. (2020). From traditional to laser cleaning techniques of parchment manuscripts: A review. *Advanced Research in Conservation Science*. 1 (1): 52-76.

**[65]** Smith, C., Paterson, R., Lowe, B., et al. (2018). Consolidation of black-dyed Māori textile artefacts: evaluating the efficacy of sodium alginate. *Studies in Conservation*. 63: 139-154.